Functional Asymmetry of the Human Na^+/Glucose Transporter (hSGLT1) in Bacterial Membrane Vesicles†

Matthias Quick, Jelena Tomasevic, and Ernest M. Wright*

Department of Physiology, David Geffen School of Medicine at UCLA, Los Angeles, California 90095-1751

Received May 20, 2003; Revised Manuscript Received June 11, 2003

ABSTRACT: The functional characteristics of the forward and reverse transport modes of the human Na^+/glucose transporter (hSGLT1) were investigated using plasma membrane vesicles of *E. coli* expressing the recombinant transporter. Correctly and inverse-oriented vesicles were employed to measure the initial rates of methyl-α-D-glucose uptake, under zero-trans conditions, as a function of Na^+, sugar, and phlorizin concentrations and membrane potential. This approach enabled the analysis of the two faces of hSGLT1 in parallel, revealing the reversibility of Na^+/sugar cotransport. While the key characteristics of secondary active sugar transport were maintained in both modes, namely, Na^+ and voltage dependence, the kinetic properties of the two sides indicated a functional asymmetry of the transporter. That is, the apparent affinity for sugar and driver cation Na^+ exhibited a difference of more than 1 order of magnitude between the two modes. Furthermore, the selectivity pattern of ligands and the interaction of the transporter with the competitive inhibitor phlorizin were different. Whereas the high-affinity substrates, D-glucose and D-galactose, inhibited uptake of radioactive sugar tracer at their physiological concentrations (10 mM) in the forward reaction, they were poor inhibitors even at high concentrations in the reverse transport mode. Taken together, these results confirm the successful employment of *E. coli* to express and characterize a human membrane protein (hSGLT1), elucidating the functional asymmetry of this cotransporter.

Transport proteins mediate the exchange of nutrients, ions, and metabolites across the cell membrane ensuring a constant supply of energy needed for cellular survival. Cotransport proteins (cotransporters or symporters) use the free energy released from the translocation of ions down their electrochemical potential gradients as the driving force for the intracellular accumulation of their substrates. As perfect molecular machines, these cotransporters are reversible, and the direction of transport depends only on the electrochemical potential gradients of the driver cations and substrates (for a review see ref *1*). The archetype of Na^+-dependent cotransport is the Na^+/glucose transporter (SGLT1),[1] which uses the Na^+ electrochemical potential difference across the brush border membrane of the intestine and proximal renal tubule to drive the intracellular accumulation of glucose (*2*).

Functional properties of SGLT1 have been extensively explored in native tissue (*3*), brush-border membrane vesicles (*4*), *Xenopus laevis* oocytes (*5*), COS-7 cells (*6*), Sf9 cells (*7*), and CHO cells (*8*). Furthermore, a recombinant hSGLT1 was functionally expressed in *Escherichia coli*, purified to apparent homogeneity, and characterized in proteoliposomes (*9*). All of these studies assess functional properties of the forward transport mode, i.e., from outside to inside, and address ligand kinetics of the external side of the cotransporter. To date, only limited information is available on the reverse transport mode, i.e., from inside to outside, and the kinetic characteristics of the cytoplasmic side of SGLT1 (*10*, *11*).

In the present study, we have explored the functional properties of hSGLT1 expressed in bacteria and have taken advantage of the fact that right-side-out (RSO) and inside-out (ISO) plasma membrane vesicles can be prepared from bacterial cells. This approach enabled a comparative analysis of the two faces of hSGLT1 with respect to their configuration in the cell membrane, confirming the functional reversibility of the cotransport and revealing the functional asymmetry of the transporter.

EXPERIMENTAL PROCEDURES

Chemicals. Methyl-α-D-[U-^{14}C]glucopyranoside (301 μCi/μmol) (αMDG) was purchased from Amersham Biosciences. All chemicals used were of analytical grade and purchased from commercial sources.

Vesicle Preparation. Expression of recombinant hSGLT1 (hSGLT1ΔN-GFP) in *E. coli* BL21 [F^- *ompT hsdS*$_B$(r_B^- m_B^-) *gal dcm*] was achieved as described (*9*). Cells transformed with pT7−5 (*12*), which is the parental plasmid for the hSGLT1ΔN-GFP expression vector, served as a control. After growth, cells were harvested and washed in 100 mM potassium phosphate buffer, pH 7.5. Right-side-out (RSO) membrane vesicles were prepared (*13*) and resuspended in 100 mM potassium phosphate buffer, pH 7.5 at a final protein

† Supported by National Institutes of Health Grant DK19567 to E.M.W.

* To whom correspondence should be addressed. Phone: 310-825-6905. Fax: 310-206-5886. E-mail: ewright@mednet.ucla.edu.

[1] Abbreviations: αMDG, methyl-α-D-glucopyranoside; D-Glc, D-glucose; D-Gal, D-galactose; 2DOglc, 2-deoxy-D-glucose; 3OMglc, 3-*O*-methyl-D-glucose; (h)SGLT1, (human) Na^+/glucose transporter; hSGLT1ΔN-GFP, engineered hSGLT1 in which N-terminal amino acid residues 12−28 were deleted, a FLAG epitope was introduced, and a glycophorin A transmembrane span and the green fluorescence protein were fused to the C terminus; ISO, inside-out; RSO, right-side-out.

10.1021/bi034842x CCC: $25.00
Published on Web 07/11/2003

concentration of ~20 mg/mL. Inside-out (ISO) membrane vesicles were prepared by a passage of the cell suspension (5 mg wet weight/mL) through an Aminco French Press at 800 psi (*14*, *15*). Prior to the passage through the French Press, nucleic acids were degraded by the incubation of the cell suspension with 0.5 mg/mL of each DNaseI and RNaseA (Sigma) at 4 °C for 30 min. Debris and unbroken cells were removed by centrifugation at 10 000 × *g* × 15 min at 4 °C. ISO membrane vesicles were sedimented by ultracentrifugation at 160 000 × *g* × 90 min at 4 °C, washed, and resuspended in 100 mM potassium phosphate buffer, pH 7.5 at a final protein concentration of ~20 mg/mL. Phenylmethylsulfonylfluoride (0.5 mM) and protease inhibitor cocktail (Sigma) were added at all steps to reduce proteolysis.

Transport Assays. Tracer uptake of ^{14}C-αMDG by RSO and ISO membrane vesicles was performed by a rapid filtration method (*16*). The transport assay buffer contained 2 mM KCl, 1 mM $MgCl_2$, 10 mM HEPES-Tris, pH 7.5, plus either 100 mM Na^+ or choline$^+$ chloride unless otherwise indicated. For the determination of Na^+ dependence of the initial rate of αMDG uptake, equimolar replacement of Na^+ with choline$^+$ was performed to achieve Na^+ activation from 0 to 100 mM (*17*). The transport reaction was initiated by adding 50 μM ^{14}C-αMDG (at a specific activity of 20 μCi/μmol) unless indicated otherwise. The reaction was terminated by the addition of ice-cold 100 mM LiCl/100 mM potassium phosphate, pH 6.0, and filtered immediately through a 0.75 μm borosilicate GF75 microfiber filter (Advantec MFS, Inc.). Nitrocellulose filters with pore sizes of 0.45 μm and 0.22 μm (Millipore) were initially used but abandoned because of slow filtration rates. By measuring the protein amount in the filtrate (*18*), protein retention in the borosilicate filters was determined to be 90% for RSO and ISO vesicles under our experimental conditions. In contrast to a previous report (*14*), efficient filtration of ISO vesicles with the borosilicate microfiber filters was therefore possible without the addition of flocculating agents. In each experiment, a control uptake assay (50 μM αMDG in the presence of 100 mM Na^+) was performed. All experiments were repeated at least in triplicate unless otherwise specified, and errors indicate the SEM. Errors of kinetic constants represent the SE of the fit.

Analytical Methods. Protein was assayed according to a modified Lowry method (*19*), using bovine serum albumin as standard.

RESULTS

hSGLT1-Specific Na^+-Dependent Sugar Uptake. Figure 1 shows Na^+- and time-dependent uptakes of ^{14}C-αMDG by right-side-out (RSO; Figure 1A) and inside-out (ISO; Figure 1B) membrane vesicles of *E. coli* BL21 harboring recombinant hSGLT1 (hSGLT1ΔN-GFP) (*9*). In the presence of 100 mM Na^+, the initial rates of αMDG uptake by RSO and ISO vesicles after 10 s showed an 11-fold and 6-fold increase, compared to the uptakes in the absence of Na^+. Na^+-dependent sugar transport peaked within 10 min at 3.8 and 2.6 nmol αMDG per mg of total membrane protein for RSO and ISO vesicles before falling to the concentration equilibrium (>5 h). Uptake of αMDG was due to the activity of hSGLT1 in the vesicle membrane because no uptake was detectable in RSO or ISO vesicles of the same strain carrying the control plasmid (data not shown).

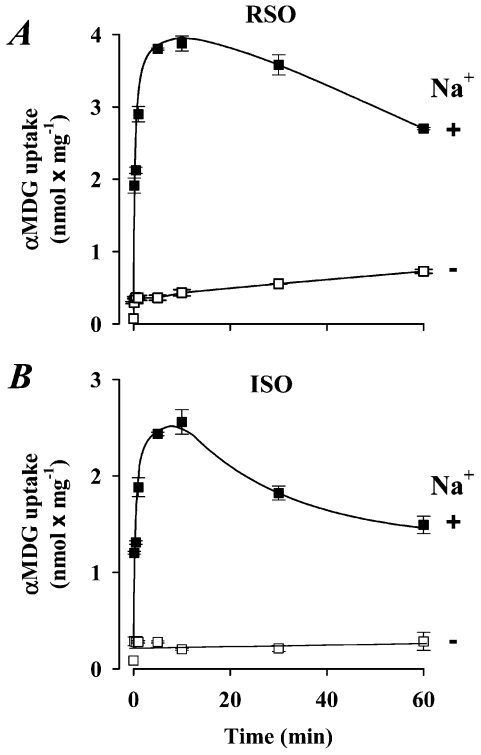

FIGURE 1: Time course of αMDG uptake by right-side out and inside-out vesicles. Uptake of 50 μM ^{14}C-αMDG (20 μCi/μmol) by (A) right-side-out (RSO) and (B) inside-out (ISO) vesicles of *E. coli* BL21 harboring recombinant hSGLT1ΔN-GFP was assayed at 22 °C. Uptakes were measured in the presence of 100 mM sodium (■) or choline (□) chloride.

Vesicle Orientation. To confirm the orientation of RSO and ISO vesicles Na^+-coupled αMDG uptake was measured in the presence of D-lactate or ATP. Addition of 5 mM D-lactic acid or Mg-ATP to the uptake buffer reduced αMDG uptake by ISO vesicles by 85% (Figure 2B). Whereas the inhibition due to D-lactic acid persisted after 30 min, the inhibitory effect of ATP was partially eliminated, reaching 57% of the uptake value in the absence of ATP. The inhibition of αMDG uptake by ISO vesicles can be attributed to the proton electromotive force ($\Delta\tilde{\mu}_{H^+}$) (interior positive and acidic) generated by the F_oF_1 ATPase or by respiration (*14*, *20*). The accessibility of the ATP-hydrolyzing part (F_1) to impermeant Mg-ATP only occurs in inverted plasma membrane vesicles. Similarly, intravesicular acidification due to the unidirectional H^+ translocation by respiration occurs only when the membrane vesicles are in the inside-out orientation. These results confirmed that the orientation of the ISO membrane vesicles was indeed inside-out. The addition of Mg-ATP or D-lactic acid had no significant effect on Na^+-dependent sugar transport by RSO vesicles (Figure 2A), implying that the RSO vesicles were also in the correct orientation.

Substrate Kinetics. The sugar selectivity of recombinant hSGLT1 in RSO and ISO vesicles was assessed by the competition of 50 μM ^{14}C-αMDG uptake with nonradioactive sugars. Addition of 10 mM αMDG, D-Glc, and D-Gal inhibited Na^+-dependent uptake of ^{14}C-αMDG by RSO membrane vesicles by 90%, while 10 mM 2DOglc did not show significant inhibition (Figure 3A). Since radiotracer uptake by ISO membrane vesicles was only slightly affected by 10 mM nonlabeled sugar (data not shown), we increased

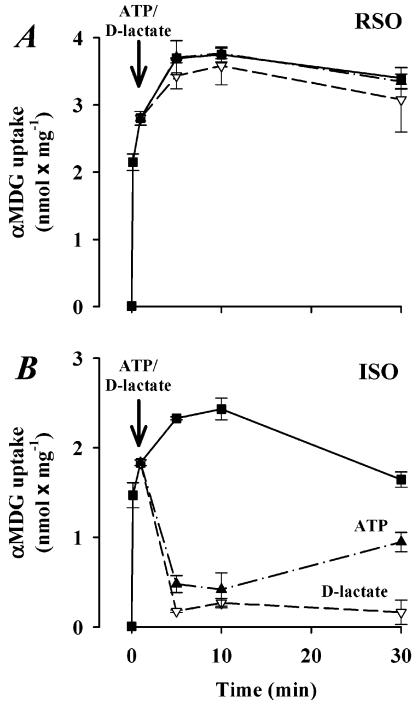

FIGURE 2: Effect of D-lactate and ATP on sugar uptake by right-side-out and inside-out vesicles. Uptake of 50 μM ^{14}C-αMDG by (A) right-side-out and (B) inside-out vesicles was analyzed in 100 mM NaCl assay buffer as described in the legend to Figure 1. When indicated (arrow), 5 mM D-lactic acid (▽) or 5 mM magnesium-ATP (▲) was added to the uptake buffer.

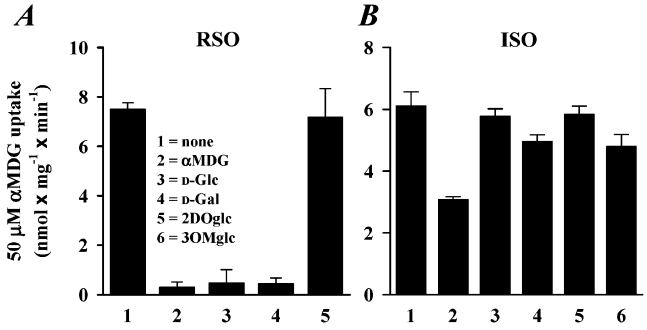

FIGURE 3: Sugar specificity of sugar transport. Initial rates of 50 μM ^{14}C-αMDG (20 μCi/μmol) uptake were measured for 10 s in 100 mM NaCl assay buffer in the presence or absence of the indicated sugar. For right-side-out vesicles (A) the concentration of methyl-α-D-glucose (αMDG), D-glucose (D-Glc), D-galactose (D-Gal), and 2-deoxy-D-glucose (2DOglc) was 10 mM ($n = 3$), while for inside-out vesicles (B), the concentration of the above sugars plus 3-*O*-methyl-D-glucose (3OMglc) was 100 mM ($n = 6$; $p < 0.01$). Mannitol (10 mM in panel A, 100 mM in panel B) was used as an osmotic control. Uptakes in its presence or absence were indistinguishable ($p < 0.01$).

the nonradioactive sugar concentrations to 100 mM. Figure 3B shows that uptake of ^{14}C-αMDG was inhibited ~50% by 100 mM αMDG and to a lesser extent by 100 mM D-Gal and 3OMglc. However, 100 mM D-Glc and 2DOglc did not inhibit the uptake of the radioactive tracer. Mannitol (10 or 100 mM for RSO or ISO vesicles), used as an osmotic control, did not inhibit sugar uptake ($p < 0.01$).

The initial rate of αMDG transport into RSO membrane vesicles after 5 s revealed a saturable function of the αMDG concentration. In 100 mM Na^+, the half-maximum saturation constant ($K_{0.5}^{\alpha MDG}$) was 0.15 ± 0.05 mM, and the maximum velocity ($V_{max}^{\alpha MDG}$) was 20 ± 2 nmol ×mg^{-1} ×min^{-1} (Figure 4A, Table 1). Similarly, uptake of αMDG by ISO vesicles exhibited saturation kinetics, with a $K_{0.5}^{\alpha MDG}$ of 56 ± 9 mM and a $V_{max}^{\alpha MDG}$ of 9 ± 1 μmol ×mg^{-1} ×min^{-1} (Figure 4B). Furthermore, indicative of cotransport, Na^+-dependent sugar transport was a function of the Na^+ concentration (Figure 5). The data showed a satisfactory fit to the Michaelis−Menten equation, exhibiting an apparent half-maximum stimulation constant ($K_{0.5}^{Na^+}$) of 1.3 ± 0.5 mM in RSO membrane vesicles and 12 ± 4 mM in ISO membrane vesicles (Figure 5A,B, Table 1).

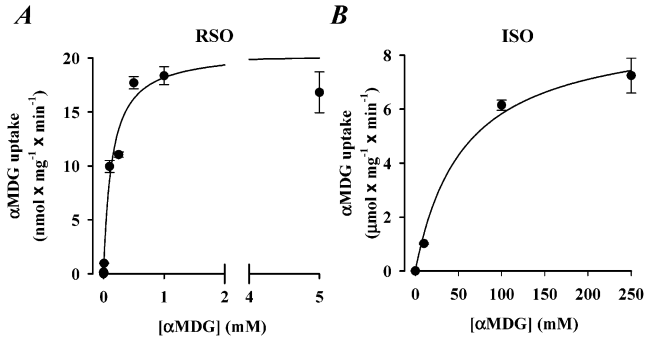

FIGURE 4: Kinetics of αMDG uptakes. Initial rates of αMDG uptakes by (A) right-side-out and (B) inside-out vesicles were measured for 5 s in 100 mM NaCl assay buffer. For right-side-out vesicles (A), the concentration of αMDG was varied between 0.01 and 5 mM. The concentration-dependence showed saturation kinetics with a half-saturation constant ($K_{0.5}^{\alpha MDG}$) of 0.15 ± 0.05 mM and a maximum velocity ($V_{max}^{\alpha MDG}$) of 20 ± 2 nmol × mg^{-1} × min^{-1}. For inside-out-vesicles (B), the αMDG concentration dependence between 0.05 and 250 mM showed a $K_{0.5}^{\alpha MDG}$ of 56 ± 9 mM and a $V_{max}^{\alpha MDG}$ of 9 ± 1 μmol mg^{-1} min^{-1}.

Inhibition. Phlorizin is a potent high-affinity competitive inhibitor of sugar transport by SGLT1 in native tissue, brush-border membrane vesicles, *Xenopus* oocytes, and reconstituted into proteoliposomes (*3*, *4*, *21*, *9*) with a half-maximum inhibition constant ($K_i^{phlorizin}$) in the micromolar range. In our study, 10 μM phlorizin inhibited the initial rate of αMDG transport by RSO vesicles by 85%, whereas the same concentration failed to inhibit uptake by ISO vesicles (Figure 6A). However, when ISO vesicles were preincubated in the presence of 10 μM phlorizin for time periods of more than 30 min, transport of αMDG was reduced to a similar level as that observed in RSO vesicles. This inhibition was time-dependent and exhibited a half-time constant (τ) of 5.2 ± 0.5 min (Figure 6B). Uptake of 50 μM ^{14}C-αMDG by RSO vesicles was inhibited by phlorizin in a concentration-dependent manner with an apparent half-maximum inhibition constant ($K_i^{phlorizin}$) of 1.9 ± 0.2 μM (Table 1).

Membrane Potential. The effect of changing the membrane potential ($\Delta\psi$) on the initial rate of Na^+-coupled αMDG uptake by RSO and ISO vesicles was analyzed (Figure 7). $\Delta\psi$ was imposed by a potassium diffusion gradient mediated by the ionophore valinomycin (*22*). Upon dilution of the vesicles (preloaded with 100 mM potassium [K^+_{in}]) into assay buffer with a lower potassium concentration, i.e., [K^+_{out}] < [K^+_{in}], the positively charged potassium ion diffused out of the vesicles down its concentration gradient. According to the Nernst-equation, $\Delta\psi$ (inside negative) was 59 and 118 mV for a 10- and 100-fold change in the [K^+_{out}]-to-[K^+_{in}] ratio. The initial rate of Na^+/αMDG cotransport by RSO vesicles after a 100-fold reduction in [K^+_{out}]

Table 1: Comparison of Kinetics of hSGLT1 Analyzed in *Xenopus* Oocytes and *E. Coli* Plasma Membrane Vesicles[a]

		bacterial vesicles	
	oocytes	right-side-out	inside-out
$K_{0.5}^{\alpha MDG}$ (mM)	0.7 ± 0.04 (21)	0.15 ± 0.05	56 ± 9
$K_{0.5}^{Na^+}$ (mM)	2.8 ± 0.2 (17)	1.3 ± 0.5	12 ± 4
$K_i^{phlorizin}$ (μM)	0.2 ± 0.01 (21)	1.9 ± 0.2	—[b]
sugar selectivity (in decreasing apparent affinity)	αMDG ≈ D-Glc ≈ D-Gal ≫ 3OMglc ≫ 2DOglc (21)	αMDG ≈ D-Glc ≈ D-Gal ≫ 2DOglc	αMDG ≫ D-Gal ≈ 3OMgl ≈ D-Glc ≈ 2DOglc

[a] Kinetic constants ($K_{0.5}^{\alpha MDG}$, $K_{0.5}^{Na+}$, and $K_i^{phlorizin}$) for recombinant hSGLT1 in bacterial membrane vesicles were obtained from measurements repeated at least in triplicate, and the error indicates the S.E. of the fit. Kinetic constants for hSGLT1 analyzed in oocytes (determined at a membrane potential of −150 mV) were taken from references as indicated. [b] Not measurable.

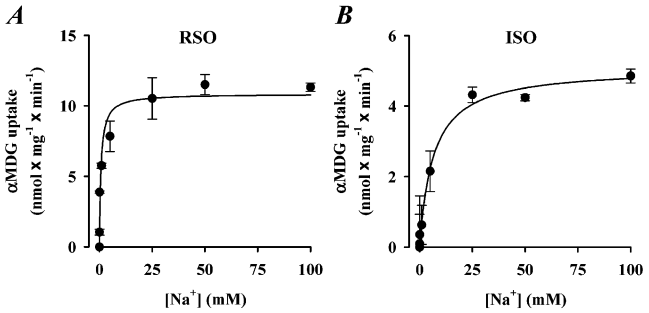

FIGURE 5: Na^+-dependence of sugar uptake. Initial rates of 50 μM ^{14}C-αMDG uptake were measured for 5 s in the assay buffer containing varying concentrations of Na^+ (equimolar replacement of sodium with choline to a total concentration of 100 mM). Upon variation of the Na^+ concentration from 0.1 to 100 mM, the apparent half-maximum concentration constant ($K_{0.5}^{Na+}$) for recombinant hSGLT1 was 1.3 ± 0.5 mM for right-side-out vesicles (A) and 12 ± 4 mM for inside-out-vesicles (B).

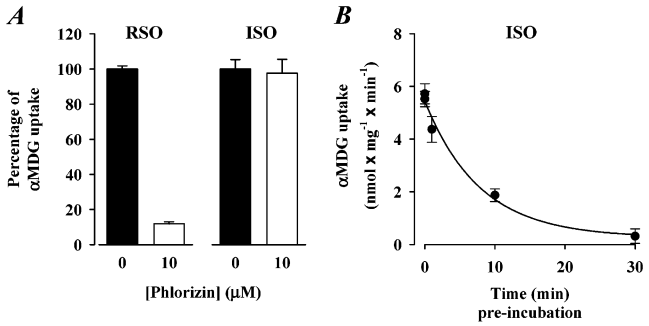

FIGURE 6: Effect of phlorizin on sugar uptake. Initial rates of 50 μM ^{14}C-αMDG uptake by right-side-out and inside-out vesicles were measured for 10 s in 100 mM NaCl assay buffer. (A) Inhibition of the initial uptake rate by the addition of 10 μM phlorizin immediately prior to the start of the uptake reaction was observed only for right-side-out vesicles but not for inside-out-vesicles. (B) Preincubation of inside-out vesicles with 10 μM phlorizin at 22 °C inhibited the uptake activity in a time-dependent manner with a half time constant (τ) of 5.2 ± 0.5 min.

increased by 25%, from 12 to 17 nmol αMDG × mg^{-1} × min^{-1}, when the external potassium concentration was reduced from 100 to 1 mM (Figure 7A). A similar result was observed for ISO vesicles under the same experimental conditions (Figure 7B), showing a ∼ 15% increase in the initial rate of Na^+-coupled αMDG uptake at a theoretical 118 mV membrane potential difference.

DISCUSSION

In this study we have exploited a bacterial expression system for the functional characterization of a recombinant

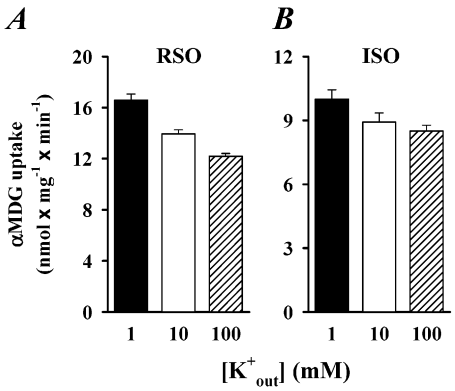

FIGURE 7: Effect of the membrane potential. (A) Right-side-out and (B) inside-out vesicles, preloaded with 100 mM potassium phosphate, pH 7.5 (see Experimental Procedures), were diluted into 100 mM NaCl assay buffer containing 1, 10, or 100 mM potassium phosphate (equimolar replacement of potassium phosphate with choline to reach a total of 100 mM). 1 μM of the potassium ionophore valinomycin was added 30 s prior to the start of the transport reaction at 22 °C to generate an inwardly directed negative membrane potential ($\Delta\psi$) in cases where the external potassium concentration ($[K^+_{out}]$) was lower than the vesicular internal concentration, i.e., below 100 mM. Initial rates of 50 μM ^{14}C-αMDG uptake were measured for 10 s ($p < 0.01$).

human Na^+/glucose transporter (hSGLT1) in plasma membrane vesicles. Our data indicate that recombinant hSGLT1 in right-side-out (RSO) bacterial membrane vesicles possessed similar kinetics of the transporter in native tissue, brush-border membrane vesicles, and *Xenopus* oocytes (*2*). That is, the uptake of ^{14}C-αMDG (a) exhibited a strict Na^+-dependence, (b) was time-dependent with an overshoot at ∼10 min before reaching the concentration equilibrium, (c) revealed a $K_{0.5}^{\alpha MDG}$ of 0.15 ± 0.05 mM and a $K_{0.5}^{Na+}$ of 1.3 ± 0.5 mM, (d) was specifically blocked by high-affinity ligands (D-glucose, D-galactose) and a competitive inhibitor (phlorizin), whereas low-affinity compounds, such as 2-deoxy-D-glucose, failed to significantly inhibit transport, and (e) showed an apparent $K_i^{phlorizin}$ of 2 μM. Furthermore, Na^+-coupled αMDG cotransport was enhanced at hyperpolarizing membrane potentials, i.e., a more negative voltage on the inside of the RSO vesicles. Taken together, these results reveal that recombinant hSGLT1 retained its mechanistic features when produced in bacteria. In addition, the kinetics of hSGLT1ΔN-GFP in RSO vesicles paralleled those reported for the purified transporter reconstituted into proteoliposomes (*9*). These results confirm that a eukaryotic membrane protein may be successfully expressed and studied in bacterial cells.

A novel aspect of the present study was the use of inverted plasma membrane vesicles of *E. coli* expressing recombinant hSGLT1 for functional assays. This unique feature allowed access to the hitherto hidden cytoplasmic face of the transporter and enabled the analysis of the reverse transport mode of hSGLT1. The results demonstrate the reversibility of Na^+-driven sugar cotransport by hSGLT1; however, there are distinct differences in the transport kinetics between the forward and the backward transport reactions.

To assess the correct orientation of the inverted plasma membrane vesicles from bacteria, we tested the sensitivity of Na^+-coupled sugar cotransport toward a reverse-oriented proton-electromotive force, $\Delta\tilde{\mu}_{H^+}$ (interior positive and acidic) (*20*). Intact cells or right-side-out vesicles pump out H^+ by means of respiration (electron transport chain) and F_1F_o ATPase-mediated transport due to ATP-hydrolysis, thus generating $\Delta\tilde{\mu}_{H^+}$ (interior negative and alkaline). $\Delta\tilde{\mu}_{H^+}$ serves as energizing force for many cellular processes, but in the context of the present report it is noteworthy to emphasize its driving power for endogenous secondary active transport systems, such as the lactose permease of *E. coli* (*1*). It has been demonstrated that inverted *E. coli* membrane vesicles can pump H^+ unidirectionally into the intravesicular space by means of respiration- and F_1F_o ATPase-catalyzed import (*14*, *20*). A prerequisite for the latter reaction is the accessibility of the ATP-hydrolyzing F_1 part of the ATPase to ATP. As a consequence of the acidification of the internal vesicle compartment, the resulting $\Delta\tilde{\mu}_{H^+}$ could eliminate or inhibit the Na^+ motive force ($\Delta\tilde{\mu}_{Na^+}$), the driving power for Na^+/sugar cotransport. Upon addition of D-lactate or Mg-ATP, Na^+-dependent αMDG transport was inhibited only in the case of ISO vesicles (Figure 2B), thus confirming the inverted orientation of the ISO vesicles.

Similar to the forward transport reaction analyzed in RSO vesicles, recombinant hSGLT1-mediated uptake of αMDG by ISO vesicles was Na^+-dependent. This result implied that when functioning in the reverse mode, the transporter also required the coupling cation for activity, thus arguing against the notion of sugar "slippage", i.e., sugar uniport, which does not require Na^+ (*23*). Supportive of this interpretation is the fact that the initial rate of αMDG transport was enhanced by increasing Na^+ concentrations with a $K_{0.5}^{Na+}$ of 12 ± 4 mM. The fact that in giant excised inside-out patches of oocytes expressing rabbit SGLT1 sugar-induced currents were observed only in the presence of Na^+ also suggests coupling of fluxes in the reverse cotransport mode catalyzed by SGLT1 (*10*, *11*). In addition to the Na^+-dependence, αMDG transport by ISO vesicles was also voltage-dependent. As shown in Figure 7B, a theoretical membrane potential difference of 118 mV (ISO vesicle interior negative and alkaline) increased the initial rate of Na^+-coupled αMDG cotransport by ~15%. This result supports previous electrophysiological observations that in giant excised inside-out patches the cytoplasmic side of the transporter exhibits a higher apparent affinity for Na^+ and/or sugar at more positive potentials (*10*, *11*).

While the major characteristics of Na^+-coupled sugar cotransport in the forward and reverse transport reactions were maintained, there were several kinetic differences. In agreement with the published data (*17*, *24*), the $K_{0.5}^{Na+}$ in the forward reaction was about 1 mM, whereas it was 10-fold lower in the opposite transport mode. A similar tendency was observed for the affinity of recombinant hSGLT1 for αMDG. The $K_{0.5}^{\alpha MDG}$ for the backward transport (56 mM) was ~350-fold higher than the $K_{0.5}^{\alpha MDG}$ for the forward uptake reaction (0.15 mM). It is not surprising that the differences in the forward and reverse $K_{0.5}^{\alpha MDG}$ are accompanied by a comparable difference in the two $V_{max}^{\alpha MDG}$ (~400-fold). According to the Haldane equation of reversible enzyme reactions, the equilibrium constant is 1 (*25*), which is in good agreement with a calculated 0.8 in our case. However, the $K_{0.5}^{Na+}$ and $K_{0.5}^{\alpha MDG}$ of hSGLT1 analyzed in *Xenopus* oocytes varies with the applied membrane potential (*17*, *21*, *24*), and we note that the results reported here were performed under nonclamped conditions. These differences in the (apparent) affinities for the ligands, along with the voltage (membrane potential) dependence, favor the forward transport mode under physiological conditions, i.e., at interior negative membrane potentials and low intracellular Na^+ concentrations.

Moreover, a marked difference between the two sides of hSGLT1 existed in the effect of ligand recognition. When admitted simultaneously with the radioactive sugar tracer, the competitive inhibitor phlorizin blocked αMDG uptake by RSO vesicles with an apparent $K_i^{phlorizin}$ of ~ 2 μM (Table 1). Under the same experimental conditions, no such effect was observed for ISO vesicles even at a phlorizin concentration of 250 μM (not shown), which is consistent with a higher $K_{0.5}^{\alpha MDG}$ in ISO vesicles. Here, inhibition of sugar transport by phlorizin was a time-dependent reaction with τ of 5.2 ± 0.5 min (Figure 5B). This result may be interpreted in two ways: (a) phlorizin binding to the cytoplasmic side of hSGLT1 exhibited a slow binding on rate, or (b) its site of action was the external face of the transporter (hidden in the ISO vesicles) after its transport across the membrane.

Furthermore, the two sides of hSGLT1 possessed different sugar selectivity patterns (Figure 3, Table 1), indicating structural differences in the sugar binding/unbinding site(s) of hSGLT1. Consistent with previous findings in oocytes (*21*), in RSO vesicles the order of decreasing apparent sugar affinity was αMDG ≈ D-Glu ≈ D-Gal ≫ 2DOglc, whereas in ISO vesicles it was αMDG ≫ 3OMglc ≈ D-Gal > D-Glu ≈ 2DOglc. This pattern is supported by the difference in the $K_{0.5}^{\alpha MDG}$ measured in RSO and ISO vesicles (see above). Remarkably, D-glucose—the physiological substrate of hSGLT1 which shares similar uptake kinetics with the nonmetabolized sugar αMDG—failed to significantly inhibit uptake of ^{14}C-αMDG even at a concentration of 100 mM (Figure 3B). Similarly, the other high-affinity substrate of hSGLT1, D-galactose, showed only a limited inhibitory effect which was comparable to that of 3-*O*-methyl-D-glucose, the latter of which exhibits a ~10-fold increased apparent affinity compared to αMDG or D-Glc in the forward mode (*21*).

Taken together, the present work revealed the functional asymmetry of recombinant hSGLT1 by exploiting the bacterial expression system. The data confirms the reversibility of hSGLT1-mediated Na^+/sugar cotransport. Under physiological conditions the functional asymmetry of hSGLT1 favors the uptake of D-glucose from the intestinal lumen into the enterocyte. This efficiency is not only gained by the Na^+ electrochemical potential gradient or the mem-

brane potential exclusively, but also by the different structural arrangement of the ligand binding site(s) on both sides of the transporter.

ACKNOWLEDGMENT

We thank Drs. H.R. Kaback and L. Guan for their help with the French Press.

REFERENCES

1. Kaback, H. R., Sahin-Tóth, M., and Weinglass, A. B. (2001) *Nat. Rev. Mol. Cell Biol. 2*, 610−620.
2. Wright, E. M. (2001) *Am. J. Physiol. 280*, F10−F18.
3. Schultz, S. G., and Curran, P. F. (1970) *Physiol. Rev. 50*, 637−718.
4. Ikeda, T. S., Hwang, E. S., Coady, M. J., Hirayama, B. A., Hediger, M. A., and Wright, E. M. (1989) *J. Membr. Biol. 110*, 87−95.
5. Hediger, M. A., Coady, M. J., Ikeda, T. S., and Wright, E. M. (1987) *Nature 330*, 379−381.
6. Birnir, B., Lee, H.-S., Hediger, M. A., and Wright, E. M. (1990) *Biochim. Biophys. Acta 1048*, 100−104.
7. Smith, C. D., Hirayama, B. A., and Wright, E. M. (1992) *Biochim. Biophys. Acta 1104*, 151−159.
8. Lin, J.-T., Kormanec, J., Wehner, F., Wielert-Badt, S., and Kinne, R. K.-H. (1998) *Biochim. Biophys. Acta 1373*, 309−320.
9. Quick, M., and Wright, E. M. (2002) *Proc. Natl. Acad. Sci. U.S.A. 99*, 8597−8601.
10. Sauer, G. A., Nagel, H., Koepsell, H., Bamberg, E., and Hartung, K. (2000) *FEBS Lett. 469*, 98−100.
11. Eskandari, S., Loo, D. D. F., and Wright, E. M. (1999) *FASEB J. A399*.
12. Tabor, S., and Richardson, C. C. (1985) *Proc. Natl. Acad. Sci. U.S.A. 82*, 1074−1078.
13. Kaback, H. R. (1971) *Methods Enzymol. 22*, 99−120.
14. Lancaster, J. R., Jr., and Hinkle, P. C. (1977) *J. Biol. Chem. 252*, 7657−7661.
15. Vázquez-Ibar, J. L., Weinglass, A. B., and Kaback, H. R. (2002) *Proc. Natl. Acad. Sci. U.S.A. 99*, 3487−3492.
16. Quick, M., and Jung, H. (1998) *Biochemistry 37*, 13800−13806.
17. Quick, M., Loo, D. D. F., and Wright, E. M. (2001) *J. Biol. Chem. 276*, 1728−1734.
18. Hirayama, B. A., and Wright, E. M. (1986) *Pflügers Arch. 407*, S174−S179.
19. Peterson, G. L. (1977) *Anal. Biochem. 83*, 346−356.
20. Reenstra, W. W., Patel, L., Rottenberg, H., and Kaback, H. R. (1980) *Biochemistry 19*, 1−9.
21. Díez-Sampedro, A., Wright, E. M., and Hirayama, B. A. (2001) *J. Biol. Chem. 276*, 49188−49194.
22. Jung, H., Tebbe, S., Schmid, R., and Jung, K. (1998) *Biochemistry 37*, 11083−11088.
23. Firnges, M. A., Lin, J.-T., and Kinne, R. K.-H. (2001) *J. Membr. Biol. 179*, 143−153.
24. Loo, D. D. F., Eskandari, S., Boorer, K. J., Sarkar, H. K., and Wright, E. M. (2000) *J. Biol. Chem. 275*, 37414−37422.
25. Segel, I. H. (1975) Enzyme kinetics. Wiley-Intersciences, New York.

BI034842X